Applied Physics A (2018) 124:512
https://doi.org/10.1007/s00339-018-1931-8

Applied Physics A
Materials Science & Processing

Comprehensive investigation of the interfacial misfit array formation in GaSb/GaAs material system

Agata Jasik[1] · Iwona Sankowska[1] · Andrzej Wawro[2] · Jacek Ratajczak[1] · Rafał Jakieła[2] · Dorota Pierścińska[1] · Dariusz Smoczyński[1] · Krzysztof Czuba[1] · Kazimierz Regiński[1]

Received: 8 December 2017 / Accepted: 20 June 2018 / Published online: 29 June 2018
© The Author(s) 2018

Abstract

A comprehensive investigation of the interfacial misfit (IMF) array formation has been carried out. The studies were based on the static phase diagram for GaAs (001) surface and As_2 dimers on the surface. Prior to the initiation of the GaSb growth two attempts of the temperature decreasing were performed: before and after the GaAs termination. The GaAs was grown in the optimal conditions for GaSb material. The influence of the interruption time on GaSb/GaAs heterostructure parameters was examined. Two cases were investigated: with and without Sb-soaking of the GaAs surface. The periodic array of edge dislocations at GaSb/GaAs interface was confirmed using Burger's circuit theory. Careful examination of misfit surroundings revealed one uncompleted Burger's vector that indicated one dislocation of mixed type among eight of the edge type. The distance between lattice sites of dislocations was 5.51 nm on average. The crystal quality of 5.0 µm GaSb layer was characterized by $FWHM_{2\theta/\omega} = 42$ arcsec, $FWHM_{RC} = 125$ arcsec. The $EPD = 4 \times 10^6\ cm^{-2}$ was estimated after etching in $FeCl_3$:HCl solution. The $\Delta q_z/\Delta q_x$ ratio of 0.60 for 5.0 µm GaSb layer was higher than for 2.5 µm GaSb layer of 0.59. The probable reason was the thickness-dependent 60° dislocation density. The electrical parameters measured for 2.5 µm GaSb were: $p = 4.0 \times 10^{16} cm^{-3}$ ($2.0 \times 10^{16} cm^{-3}$) and $\mu = 599\ cm^2/V\ s$ ($3420\ cm^2/V\ s$) at 300 K (77 K).

1 Introduction

Type II InAs/GaSb superlattices (SLs) attract great interest in technology of the infrared (IR) photodetectors [1–3]. The most suitable substrates for the growth of these SLs are lattice-matched GaSb wafers. However, for many applications of GaAs substrates are more desirable as an inexpensive material with a small free-carrier absorption in the IR spectral region (a semi-insulating material) and favourable thermal properties. The high lattice mismatch (7.8%) between GaSb epitaxial layer and GaAs substrate hinders the growth of sophisticated device structures. Nowadays, this mismatch is accommodated either via a metamorphic buffer [4–7] or more recently, by a periodic interfacial misfit (IMF) array growth mode [8–17].

✉ Agata Jasik
ajasik@ite.waw.pl

[1] Institute of Electron Technology, Al. Lotnikow 32/46, 02-668 Warsaw, Poland

[2] Institute of Physics Polish Academy of Science, Al. Lotnikow 32/46, 02-668 Warsaw, Poland

In the IMF growth mode, the strain is relieved instantaneously at the mismatched heterointerface by the formation of a two-dimensional periodic array of pure edge dislocations. The IMF array is formed by the periodic skipping of atomic bonds, which results in a highly periodic array of Ga-dangling bonds localized at the GaSb/GaAs interface. The misfit periodicity corresponds to exactly 13 GaSb and 14 GaAs lattice sites. In this way, the strain remains localized at the interface rather than propagating in the vertical direction—dislocations propagate along two directions: [110] and [1–10]. The GaSb layer is almost completely relaxed with low dislocation density.

The first reports on IMF growth mode in GaSb/GaAs material system were presented by Rocher in 1991 [9] and Ivanov et al. in 1993 [10]. Since then the IMF has been implemented in several systems including GaP/Si [11], GaAs/Si [12], InAs/GaAs [13], InAs/GaP [14], InP/GaAs [15], AlSb/Si [16] and GaAs on GaSb [17]. However, so far this mode has not been well-established due to both unrepeatable growth under technological conditions in a narrow epitaxial window and complex characterization.

The benefits of the GaAs substrate for application in antimonide technology on one side and unrepeatable IMF

growth on the other justify the renewed efforts of many research groups to optimize this relaxation mode [18]. It is important, among other things, to make it repeatable. This will become much easier to achieve when the entire process of IMF formation will be recognized comprehensively from the GaAs substrate preparation to the GaSb growth termination.

Since the IMF formation is governed by the surface thermodynamics and kinetics, it can only be initiated on the smooth GaAs surface, at optimal temperature and under optimal conditions for the growth of GaSb layer. The search for the optimized conditions of GaSb growth, smooth GaAs layer and the proper initiation of GaSb growth on GaAs surface were main aims of the paper. The results of the experiment are optimized growth conditions of fully relaxed GaSb layer on GaAs substrate with reduced dislocation density of 4×10^6 cm^{-2}.

2 Experiment

The experiment was carried out using molecular beam epitaxy (MBE) 32P Riber machine. The growth chamber was equipped in SUMO effusion cell for Ga and valved cells with cracking zone for As and Sb elements. The temperature of cracking zones was kept constant at 1000 °C to obtain highest possible mole fraction of As_1 and Sb_1 particles guaranteeing good optical quality of the material [19]. The quality of grown layers was monitored in situ using reflection high-energy electron diffraction (RHEED). The pyrometers for the temperature measurements on both GaAs (IRCON, spectral response peak at 930 nm, 450 °C–1200 °C) and GaSb (RAYTEC, spectral response peak at about 1640 nm, 250 °C–1100 °C) material surfaces were used. The temperature was verified by the oxide desorption for GaAs material and the appearance of RHEED oscillations at $T_G < 500$°C during the GaSb growth. The homoepitaxial GaSb and GaAs layers, as well as GaSb/GaAs heterostructures were deposited on (001) non-doped GaSb and (001) Si-doped GaAs (GaAs:Si) substrates excluding samples intended to Hall measurements. In this case (001) semi-insulating material GaAs(SI) was used. The growth rate of GaAs material was determined by the Ga-flux used in the optimized growth of the GaSb material. The ratios of group V–group III elements (V/III ratio) beam equivalent pressure for GaSb and GaAs materials were established during the optimization process, as well as the growth temperature for GaSb layer. The growth temperature for GaAs material was kept constant of 580 °C.

The thermodynamic and kinetic conditions governing the IMF formation divided the experiment into three parts. The first one concerned the optimization of the GaSb growth and allowed for determination of the input Ga-flux for the second one. The latter focused on obtaining the atomically smooth surface of thin GaAs layer with reduced impurity concentration. The third part was dedicated to the commencement of GaSb growth on GaAs surface, i.e. the growth of relaxed heterostructure using IMF mode. At first the IMF mode was investigated in situ using the changes in the reflection high-energy electron diffraction (RHEED) pattern. Next GaSb/GaAs growth was optimized following the methodology developed in the previous step.

The crystal and optical quality of the samples were examined using atomic force microscopy (AFM), high-resolution X-ray diffraction (HRXRD) and reflection (HRXRR), high-resolution transmission electron microscopy (HRTEM), scanning electron microscopy (SEM) and Fourier-transform infrared spectroscopy (FTIR). The material purity was controlled by the means of secondary ion mass spectrometry (SIMS) and electrical parameters measurements using Van der Pauw method. The preliminary assessment of surface quality was made under Nomarski microscope.

2.1 Optimization of GaSb growth

During the optimization process of GaSb growth, the following main technological parameters were investigated: growth rate r_g, growth temperature T_g and V/III ratio. It was assumed that weak dependence of the growth rate on the V/III ratio did not influence the investigated parameters. The annealing and cooling conditions provided stabilisation of the Sb-surface during substrate heating and prohibited the Sb-condensation during the cooling stage after the growth termination [20]. The growth conditions and obtained results are shown in Table 1.

The AFM images show two–dimensional growth mode (2D mode) for all samples. The homoepitaxial GaSb layer with flat surface gives a chance to obtain a heteroepitaxial GaSb/GaAs layer relaxed by IMF mode. Nevertheless, some of the surfaces are undulated, which indicates the peak–to–valley parameter higher than 1 ML, two of them are well-developed with regular pyramids (#10, #11, Fig. 1). The conditions resulting in absolutely flat GaSb surface were taken into account in further optimization of GaSb/GaAs growth.

The crystal quality of only three samples #8, #13 and #18 deviates from the high standards outlined by the bulk material on the level of 22 arcsec FWHM in $2\theta/\omega$ scan. The great majority of samples exhibit high crystal quality.

The optical quality of the GaSb layers was characterized using PL measurements. The PL spectra measured at 10 K and registered for all samples are dominated by the exciton transitions: the peaks assigned to the bound–exciton (BE) transition are located at 0.796 to − 0.798 eV, while free-exciton (FE) peaks are placed at 0.807–0.809 eV [21]. The FE peak is a clear demonstration of high material quality.

Table 1 The growth conditions and obtained results for GaSb homoepitaxial layers

No.	r_g (Å/s)	T_g (°C)	V/III	AFM (nm)		HRXRD FWHM (arcsec)		I_{PL} at 10 K	$\frac{I_{FE}}{I_{PL}}$
				RMS	ptv	$2\theta/\omega$	RC		
#1	1.3	520	2.9	0.32	1.15	24.4	22.7	0.102	0.20
#2	1.3	520	3.5	0.10	0.24	20.2	12.9	0.164	0.21
#3	1.0	520	2.5	0.06	0.30	20.8	12.6	0.378	0.19
#4	1.0	520	2.9	0.09	0.26	21.1	12.8	0.256	0.15
#5	**1.0**	**520**	**3.5**	**0.11**	**0.22**	**21.6**	**14.6**	**0.378**	**0.23**
#6	1.6	520	2.9	0.07	1.03	22.9	18.7	0.378	0.26
#7	1.6	520	3.5	0.07	0.17	20.1	12.9	0.182	0.18
#8	1.3	500	2.9	0.07	0.19	21.2	14.2	0.333	0.24
#9	1.3	500	3.5	0.07	1.05	19.4	12.4	0.603	0.27
#10	1.3	480	2.9	1.10	4.19	20.9	16.5	1.0	0.19
#11	1.3	480	3.5	2.36	5.65	21.4	13.6	0.914	0.17

Labels: r_g *(Å/s)* growth rate, T_g *(°C)* growth temperature, *V/III* ratio of BEP of group V–group III, *RMS (nm)* roughness means as RMS determined from (5×5) µm AFM image analysis, *ptv (nm)* height of peak-to-valley determined from AFM images, FWHM of GaSb peak on 2theta-omega ($2\theta/\omega$) scan and rocking curve (RC) measured using HRXRD, I_{PL} *at 10 K* integrated PL intensity, normalized to unity, PL spectra have been measured at 10 K, $\frac{I_{FE}}{I_{PL}}$ the ratio of the integrated intensity of free-exciton transition to integrated PL intensity

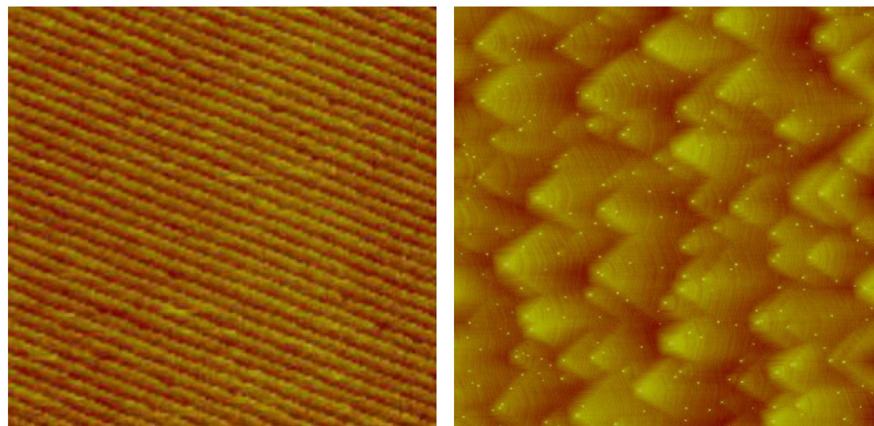

(a) 2D mode, #5 sample **(b)** 2D mode with pyramids, #11 sample

Fig. 1 (10×10) µm AFM images of GaSb homoepitaxial layers. The sample #5 has atomically flat surface (**a**) and sample #11 has well-developed surface (**b**)

Based on the fit of the measured spectra using Gaussian distribution, the contribution of FE intensity to the total PL intensity was estimated to be higher than 15% (sample #4, Table 1). There are also peaks located at 0.780–0.790 eV assigned to a donor–acceptor transitions and barely visible conduction band–acceptor transition at around 0.760 eV [19]. The direct energy gap of GaSb material is reported to be between 0.811 and 0.815 eV [21]. An exemplary PL spectrum for the sample #5 is presented in Fig. 2.

The integrated PL intensity normalized to unity, as well as the ratio of free-exciton intensity to PL intensity have been calculated for all spectra and collected in Table 1. The lowest intensity was obtained for samples grown at the highest temperature and high V/III ratio while the highest intensity was exhibited for sample deposited at the lowest temperature.

The analysis of the obtained parameters indicates that only two samples #5 and #8 have both high crystal and optical quality. They are characterized by the RMS surface roughness below 1 ML, $FWHM_{2\theta/\omega}$ narrower than 22 arcsec and relatively high PL intensity. Due to the stronger PL intensity and absolutely straight monoatomic terraces on AFM image, the parameters employed for the deposition of sample #5 were chosen as optimal for the growth of the GaSb material: growth rate of 1.0 Å/s, growth temperature of 520 °C and V/III = 3.5. Relatively small GaSb growth rate of 0.7 Å/s is considered to be optimal also by other authors [22]. They claim that optimal growth is simultaneously slow

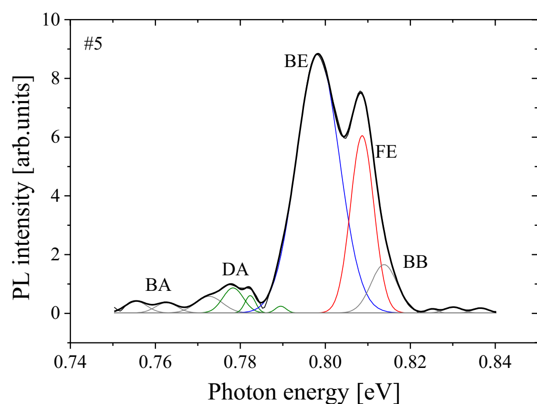

Fig. 2 PL spectra of sample #5 (GaSb homoepitaxial layer) at 10 K. From the fit of the measured spectra (black line) using Gaussian distribution the accurate peak positions and the energy values have been found. The free exciton peak have been identified at 0.809 eV (red line)

enough to provide mobility of Ga atoms and fast enough to prohibit them to reach the low-energetic sites around the defects.

Because the growth chamber is equipped with only one Ga effusion cell, the optimal growth rate of 1.0 Å/s for GaSb has defined the Ga-flux that was used for GaAs growths in further investigations.

2.2 Optimization of GaAs substrate annealing

To optimize the GaAs substrate annealing two main issues were studied: the smoothness and the impurity concentration at interface between GaAs substrate and GaAs layer. First, the native oxide was desorbed from GaAs substrate during its slow heating with the rate of 10 °C/min. Then the substrate was annealed, and after that cooled down to deposit a thin GaAs cover layer with the growth rate of 1.0 Å/s resulting from the Ga-flux applied for GaSb growth. The following annealing conditions were under investigation: the temperature of 605, 615 and 625 °C and the duration of 0, 1, 2 and 4 min. We have claimed that the thin GaAs layer "freezes" the atomic order on the substrate surface and maps it in greater extent than the substrate itself. We fixed the optimal thickness of the thin GaAs layer to be 25 nm. Thinner layers revealed the lack of coalesced material—deep holes. The impurity concentration at the GaAs substrate/GaAs layer interface was investigated for thicker layers of 500 nm. The interface smoothness was examined using AFM and HRXRR and the impurity concentration at the interface—using SIMS. Both employed annealing conditions and the obtained results are collected in Table 2.

The growth by coalescence of 2D islands was observed for all samples (Fig. 1a, b) except #18 (Fig. 1c). For this sample, 3D growth mode took place and the islands reached height of 8 nm. In the case of four other samples few holes (some of them marked in Fig. 1b) or peaks and 3D islands with a depth (height) of about 1.4 nm (7.0 and 3.5 nm) are visible between 2D islands. The pure 2D growth mode results in RMS of about 0.2 nm (Fig. 1a). The samples annealed at the temperature of 615 °C with pure 2D growth mode exhibit small peak-to-valley ratio. The acceptable annealing may be reduced to heating up the substrate to 615 °C and cooling down to the growth temperature of 580 °C. Nevertheless, the lowest roughness in both nano- (RMS) and microscale (R_S) obtained for sample #17 indicates that the optimal conditions for substrate annealing are: $T_A = 615$ °C, $t_A = 4$ min. The roughest surface in nanoscale and smoothest in microscale was observed for sample #18 annealed at 625 °C for 1 min (Fig. 3).

The similar experiment was carried out to determine the annealing conditions, which would allow for obtaining the lowest impurity concentration at the substrate/layer interface. The two possible sources of contamination should be

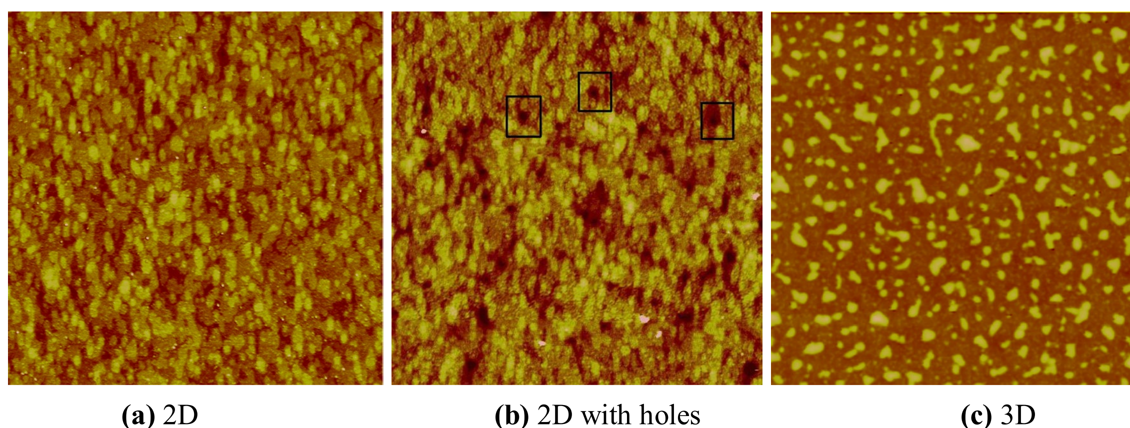

(a) 2D **(b)** 2D with holes **(c)** 3D

Fig. 3 (3 × 3) μm AFM images taken for thin GaAs layers deposited on GaAs substrate and annealed under different conditions

considered: the substrate surface with absorbed or adsorbed impurities on it and the As-flux stabilizing substrate surface during the annealing. The experiment was preceded by the growth of three 8.0 µm GaAs layers with different V/III ratio of 7.5, 8.5 and 9.5 to determine the lowest As-flux resulting in high crystal quality. The V/III ratio of 7.5 ensures stable 2 × 4 surface reconstruction, whereas value of 7.0 resulted in 4 × 2 RHEED pattern. The crystal quality as well as impurity and carrier concentration in the layers were monitored using HRXRD, SIMS and Hall measurements. Van der Pauw method was applied to estimate the electrical parameters of 1.0 cm × 1.0 cm square samples. The depletion regions located at GaAs(SI)–layer interface (~ 0.48 µm) and underneath the GaAs surface (~ 0.45 µm) were taken into account for the determination of carrier concentration. The results are collected in Table 3.

The worst crystal quality was obtained for the highest V/III ratio. The electrical parameters are comparable between the samples. The impurity concentration is lowest for highest V/III ratio, but the small differences in concentration between samples do not justify using the highest value of

Table 2 The parameters of GaAs substrate annealing and obtained results

No.	T_A (°C)	t_A (min)	AFM			HRXRR	
			RMS (nm)	ptv (nm)	Growth type	R_S (nm)	R_L (nm)
#12	615	0	0.18	0.7	2D	0.48	0.67
#13	625	0	0.24	1.4	2D with holes	0.65	0.56
#14	605	0	0.21	1.1	2D with holes	0.0	0.77
#15	615	1	0.23	0.7	2D	0.47	0.71
#16	615	2	0.24	7.0	2D with peaks	0.48	0.67
#17	**615**	**4**	**0.18**	**0.6**	**2D**	**0.28**	**0.73**
#18	625	1	1.83	8.0	3D	0.24	0.50
#19	625	2	0.20	3.5	2D with 3D	0.47	0.59
#20	605	4	0.21	1.1	2D	0.65	0.88

T_A temperature and duration, t_A time of the annealing, *RMS* roughness of the layer and *ptv* the height of the peak-to-valley obtained from (3 × 3) µm AFM images, *2D*/*3D* two/three dimensional growth, R_S/R_L the roughness determined for the substrate–layer interface/the free surface of GaAs layer using HRXRR

Table 3 The FWHM of the rocking curve (RC) and the 2theta-omega ($2\theta/\omega$) scan, impurity (carbon C and oxygen O) concentration and electrical parameters (hole concentration *p* and hole mobility *μ*) for GaAs grown at different V/III ratio

No.	V/III	HRXRD FWHM (arcsec)		SIMS I (cm^{-3})		Hall at 300 K	
		RC	$2\theta/\omega$	C	O	p (cm^{-3})	μ (cm^2/V·s)
#21	7.5	10.6	19.6	4.2×10^{16}	5.2×10^{16}	4.1×10^{15}	361
#22	8.5	10.3	20.6	3.7×10^{16}	2.9×10^{16}	4.5×10^{15}	359
#23	9.5	17.0	28.0	2.3×10^{16}	3.8×10^{16}	4.2×10^{15}	351

Table 4 Temperature T_A and time t_A of GaAs substrate annealing and parameters describing the layer quality

No.	T_A (°C)	T_A (min)	AFM RMS (nm)	HRXRD FWHM (arcsec)		SIMS $I \times 10^{13}$ (at/cm^{-2})	
				RC	$2\theta/\omega$	C	O
#24	625	1	0.46	9.1	18.9	8.8	5.3
#25	625	2	0.46	10.2	20.1	20.0	15.0
#26	625	4	0.45	13.9	24.5	13.0	9.7
#27	**615**	**0**	**0.55**	**9.8**	**19.5**	**6.1**	**2.0**
#28	615	2	0.53	9.5	19.1	71.0	3.2
#29	615	4	0.56	8.5	18.3	57.0	2.2
#30	605	1	0.98	8.9	18.6	14.0	2.6
#31	605	4	0.73	10.9	20.6	14.1	1.9

GaAs surface roughness RMS obtained from (3 × 3) µm AFM images, FWHM of rocking curve (RC) and $2\theta/\omega$ scan obtained using HRXRD and intensity of SIMS peak (I) for carbon and oxygen

As-flux for regular growths, so V/III = 8.0 was chosen for further investigations.

The most common impurities in MBE technology of arsenides were measured by SIMS and the results are collected in Table 4. The conditions considered as acceptable and optimal in the previous stage have been repeated for 500 nm layers in samples #27 and #29. The crystal and surface quality were also monitored using HRXRD and AFM techniques, respectively.

The highest roughness was observed on the surface of the sample annealed at the lowest temperature, while the samples with worst crystal quality corresponded to the highest temperature. The integrated intensity of SIMS signal was used to calculate the impurity concentration at the interface. The largest carbon concentration was measured for sample grown on the substrate annealed at medium temperature. This limited the number of samples to three: #24, #27, #29. The low impurity concentration at the interface was measured for the shortly annealed samples. The lowest one was obtained for sample #27 heated to 615 °C and then cooled down ($t_A = 0$ min). The best crystal quality, i.e. the narrowest FWHM was measured for sample #29 grown on the substrate annealed under the conditions considered to be optimal in the previous stage. Because the temperature of 625 °C is close to the congruent temperature of GaAs, precise control of the temperature during surface heating is crucial. The inaccuracy of temperature determination may threaten the surface degradation during substrate annealing. To escape from this critical point, the lower temperature of 615 °C was chosen as an optimal one but without the annealing stage ($t_A = 0$ min, sample #27).

The growth mode for 500 nm layers was 2D as was for thin 25 nm layers. In the case of the thick layers, the islands coalesced and formed narrow terraces as can be seen in Fig. 4 (Stranski–Krastanov growth mode).

Summarizing, taking into account both the smoothness and high purity of GaAs substrate/GaAs layer interface, the optimal conditions for substrate annealing are the ones used during the growth of sample #27, i.e. after oxide desorption the substrate was heated to $T_A = 615$ °C and then cooled down to 580 °C without additional annealing.

2.3 Optimization of GaSb growth on GaAs substrate by use of interfacial misfit array

2.3.1 The interfacial misfit array (IMF)

Prior to the growth of GaSb/GaAs heterostructures, many attempts at IMF mode were made. The studies were based on the static phase diagram for GaAs (001) surface and As_4 tetramers determined previously at our laboratory, Fig. 5, [23]. The phase boundaries divide the diagram into four regions with different reconstructions, except for the region of (3 × 1) reconstruction, where (3 × 6) one can also be seen. Activation energies for the phase transitions between reconstructions (2 × 4) → (3 × 1) and (3 × 1) → (4 × 2) are 3.64 eV and 3.30 eV, respectively [23].

The diagram was adopted for the experiment with As_2 dimers after an experimental verification of some transition points indicated by the solid stars in Fig. 5. For the latter, As_2 flux as before As_4 one was measured by a rotating Bayard–Alpert gauge mounted on the sample manipulator. The obtained points set new phase boundaries, which are not exactly parallel to the previous ones. As can be seen, the boundaries for As_2 fluxes larger than 1×10^{-7} Torr are shifted into a region of higher temperatures. For instance, the phase transition (3 × 1) → (4 × 2) at As_2 flux of 2.9×10^{-6} Torr is at the temperature of 715 °C while for the same flux of As_4 it is at 685 °C. In the region of low As fluxes, the boundaries are independent of the As particles

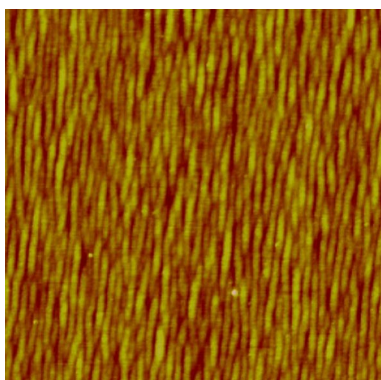

Fig. 4 (3 × 3) µm AFM image taken for 500 nm GaAs layer deposited on GaAs substrate annealed at T_A = 615 °C and t_A = 0 min (sample #27)

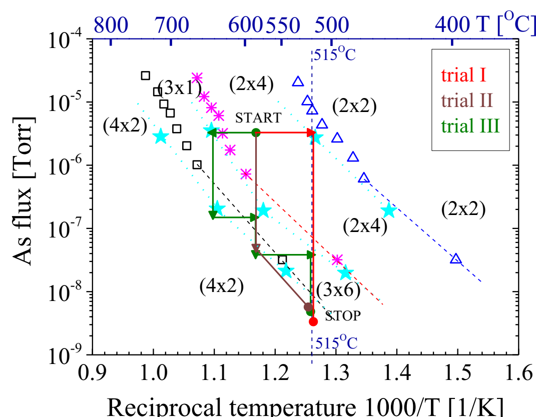

Fig. 5 The static phase diagram for GaAs(001) surface [23]. Solid stars are for As_2 dimers, others symbols are for As_4 tetramers

type. Similar observations were done for InAs material and high As fluxes by Brucker et al. [24].

To optimize the IMF mode, the experiment was divided into three trials schematically shown on the phase diagram in Fig. 5: trial I widely described in the literature [17, 24, 25], trial II with a graded reduction of temperature and lastly two-step trial III. The START point in Fig. 5 means that the growth of GaAs smoothing layer at temperature of 580 °C was completed and the STOP points (three points) mean that both the desired background in the growth chamber (As pressure) and the temperature of 515 °C were obtained.

Trial I After deposition of 0.5 µm GaAs-smoothing layer (the START point on the diagram), the temperature was decreased from 580 to 515 °C, the growth was interrupted and then As_2 pressure was reduced starting from 3×10^{-6} Torr during $t_i \in (0/20$ min). In most of the attempts the (2×4) reconstruction remained unchanged being "frozen", whereas in some of them (3×1) was observed. The (4×2) surface reconstruction rarely occurred. The GaSb growth was initiated by successive opening the cells, first Sb-shutter, then Ga-shutter. The RHEED pattern was difficult to identify during first few seconds. After that the (3×1) reconstruction appeared indicating a planar growth of relaxed material.

This trial was repeated for the case when the temperature was decreasing after finishing the GaAs growth. Next steps were the same. The surface reconstruction has been reproduced.

The results of this trial stand in a sharp contrast to those reported by other authors [17, 25, 26]. For analogous attempts they observed the incontestable transition $(2\times4)\rightarrow(4\times6)$ on RHEED images.

Trial II After deposition of 0.5 µm-GaAs smoothing layer, the temperature was kept constant at 580 °C, As-cell was closed (both shutter and valve) and at once the As flux was reduced by predetermined value (specified by t_i), the temperature was ramped down (30 °C/min) while RHEED image was being monitored. The reconstruction was usually (4×2) but at times it changed to (4×6) or even to $(3\times1, 6)$. It was hard to "freeze" the (4×2) pattern indicating Ga-terminated surface (all atoms are Ga) but in this region of parameters (the temperature, As pressure) the Ga-rich surface (most of the atoms are Ga) was easily achievable. At the temperature of 515 °C the GaSb growth was initiated as it was mentioned in Trial I. The RHEED pattern was spotty during first dozens of seconds. After that the (3×1) reconstruction appeared.

Trial I and II differed in the parameter that was reduced first: as flux or surface temperature. In trial II the temperature was decreased after the As flux has been reduced by predetermined value (determined by t_i). The transition $(2\times4)\rightarrow(3\times1, 6)$ has a higher activation energy than $(3\times1, 6)\rightarrow(4\times2)$ so it can occur easier at higher temperature. In the case, where the temperature on the surface is too low for the former transition, the (4×2) reconstruction does not appear. This is both the explanation why some reconstructions can remain "frozen" and justification for the Trial II. Nevertheless, it should be noted that during a first dozens of seconds the growth was three-dimensional, which may result in a worse crystal quality of GaSb material.

Trial III After deposition of 0.5 µm-GaAs smoothing layer, the temperature was increased from 580 to 630 °C to get (3×1) reconstruction and then As_2 pressure was reduced from 3×10^{-6} Torr by about ten times and immediately after the (4×2) reconstruction appeared, the temperature was decreased to about 580 °C. It resulted in the change of reconstruction from (4×2) to (3×1). Further reduction of both the As_2 pressure and the temperature (two steps, see the diagram in Fig. 5) was performed while taking care to stay in the diagram region of (3×1) due to the lower activation energy of the phase transition from (3×1) to (4×2) than from (2×4) to (3×1). When the temperature reached 515 °C and the As_2 has decreased to the background level (three orders of magnitude from the starting point), the (4×2) reconstruction usually occurred although the main reflexes were not always strong enough to identify them unambiguously. The growth of GaSb was initiated in the same manner as in Trial I and II. During the growth of about 9–10 MLs the RHEED image changed from a dotted one to (3×1) pattern.

This Trial was repeated for the case, in which the temperature was decreased after the completion of the GaAs growth. The rest of the procedure was analogous. The surface reconstruction has been reproduced.

Although Trial III allowed for obtaining almost "frozen" (4×2) reconstruction indicating a stable Ga-terminated GaAs surface, the lack of the group-V surface stabilization at high temperature did not allow to maintain the atomically smooth GaAs surface. It led to the roughening of free surface and resulted in three-dimensional growth of first 9–10 MLs of GaSb material.

We found Trial I to be the most applicable due to the fast transition to 2D growth ensured by the appearance of (1×3) surface reconstruction.

2.3.2 The GaSb/GaAs heterostructure with IMF

The IMF mode has been used for the strain relaxation in GaSb/GaAs heterostructures. The repeatable IMF mode requires atomically smooth GaAs surface, relatively low temperature on GaAs surface and a negligibly low partial pressure of As in a growth chamber [27]. For the growth of GaSb/GaAs heterostructures applying IMF mode the technological conditions determined in previous sub-sections were employed: thermal treatment of GaAs substrate and growth conditions of GaSb layers. Following them, after the oxide desorption, the substrate was heated up to the temperature of 615 °C and cooled down to 580 °C, stabilized and the

GaAs growth was started. After deposition of 500 nm of GaAs buffer layer, for the sample set A the temperature was lowered to 515 °C without GaAs interruption and then the growth was stopped by shutting off both Ga and As cells, whereas for the sample set B the GaAs growth was interrupted and after that the temperature was lowered to 515 °C. Next, the surface reconstruction and the partial pressure in growth chamber were monitored for several minutes t_i. During this time, the change in reconstruction and significant decrease of partial pressure occurred. This step was crucial for strain relaxation by IMF array [28], therefore, the influence of the interruption time t_i on GaSb layer quality was investigated. Then the growth of GaSb was started either by opening the Sb and Ga cells one after another ($t_{Sb}=0$ s: #32A–#35A, #37B) or by Sb-soaking of GaAs surface for $t_{Sb}=3.0$ s and then opening Ga-shutter (#36B, #38B, #39B).

The conditions for GaSb growth were as follows, the growth rate of 1.0 Å/s, the growth temperature of 520 °C and V/III ratio of 3.5. The layer thickness was about 1.0 µm for set A and varied for set B. The GaSb layers were characterized using AFM, HRXRD, PL and HRTEM. The interruption time and obtained results are collected in Table 5.

In set A, two samples labelled #33A and #36A had smaller RMS than 2.0 nm determined for (10 × 10) µm area, whereas the second one had better, both crystal and optical parameters. It is a result of Sb-soaking of GaAs surface, which led to the formation of single bonds between Sb and Ga atoms underneath, i.e. to IMF initiation [28]. In the set B, samples are rougher.

The intensity of GaSb peak in rocking curve measured for 1 µm-GaSb layer on GaAs substrate was normalized to the intensity of GaSb peak taken for 1 µm-homoepitaxial layer grown under similar conditions (sample #5, $I_{RC}=1.5\times10^7$ cps). The samples thicker than 1 µm were grown on a semi-insulating (SI) GaAs substrates to enable the measurement of electrical parameters. The crystal quality of GaAs (SI) substrate is worse than a quality of conductive bulk material, which caused lowering of the GaAs buffer quality (Table 5) and influenced the quality of GaSb layer deposited on it. The smallest FWHMs of GaSb peaks were obtained for sample #36A grown using equal interruption and Sb-soaking times of 3.0 s. The symmetric 004 reciprocal space maps (RSMs) were measured to verify the defect structure in the samples. Based on the results, the ratio of $\Delta q_z/\Delta q_x$, where Δq_z and Δq_x are FWHMs of the signal intensity distribution measured at the reciprocal lattice point in parallel and perpendicular directions to the reciprocal lattice vector was calculated to determine the type of dislocations generated at the GaSb/GaAs interfaces (Table 5). According to Kaganer and co-authors [29], the strain relaxation occurs by generation of the edge dislocations for $\Delta q_z/\Delta q_x$ ratio higher than 0.6, whereas the lower value indicates mixed type, i.e. both 90° and 60° dislocations. Furthermore, Kaganer also showed that $\Delta q_z/\Delta q_x$ depends only on Poisson's ratio ν. Theoretical value of ν for GaSb layer equals to 0.31, which corresponds to $\Delta q_z/\Delta q_x$ values of 0.64 for edge dislocations and 0.34° for 60° dislocations. From set A, the sample #36A met the abovementioned requirement of $\Delta q_z/\Delta q_x$ ratio for edge dislocations. Its high optical quality was confirmed by the presence of FE peak in PL spectrum (Fig. 6; Table 5). In contrast to the homoepitaxial GaSb layers (Fig. 2), there is a peak at 0.804–0.806 eV in the PL spectra of GaSb layers deposited on GaAs substrate, including PL spectrum obtained for sample #36A (BD peak at 0.804 eV, Fig. 6). The peak is frequently assigned to the donor–valence band exciton transition [30]. The trials to identify the element acting as the donor using SIMS analysis did not provide expected explanation. The concentrations of donor impurities in both homoepitaxial and heteroepitaxial GaSb layers were comparable. The more detailed analysis of electrical

Table 5 The interruption time (t_i), Sb-soak time (t_{Sb}) and obtained results for GaSb/GaAs heterostructures

No.	d_L (µm)	t_i/t_{Sb} (min/s)	AFM (nm)	HRXRD FWHM (arcsec)				HRXRD GaSb		I_{PL} 10 K	$\frac{I_{FE}}{I_{PL}}$
				GaAs		GaSb					
			RMS	$2\theta/\omega$	RC	$2\theta/\omega$	RC	$I_{RC}\times10^{-2}$	$\Delta q_z/\Delta q_x$		
#32A	1.0	3/0	2.90	18.5	11.0	93	316	5.32	0.58	0.780	0.26
#33A	1.0	0/0	1.82	18.3	10.4	93	291	5.81	0.60	0.818	–
#34A	1.0	15/0	2.29	18.6	10.5	89	291	5.97	0.59	1.0	–
#35A	1.0	5/0	2.32	21.2	13.7	87	289	6.23	0.58	0.854	–
#36A	**1.0**	**3/3**	**1.96**	**18.2**	**10.8**	**82**	**234**	**7.23**	**0.63**	**0.868**	**0.12**
#37B	1.0	3/0	2.26	18.4	10.7	88	299	5.63	0.58	0.953	0.17
#38B	2.5	3/3	3.00	25.0	29.0	50	160	–	0.59	–	–
#39B	5.0	3/3	2.52	23.0	16.0	42	125	–	0.60	–	–

RMS roughness of layer and *ptv* the height of peak-to-valley obtained from (10 × 10) µm AFM images, FWHM and intensity of rocking curve (RC), FWHM of $2\theta/\omega$ scan, $\Delta q_z/\Delta q_x$ obtained from reciprocal space maps (RSMs) measured using HRXRD, integrated PL intensity PL_{peak} measured at 10 K

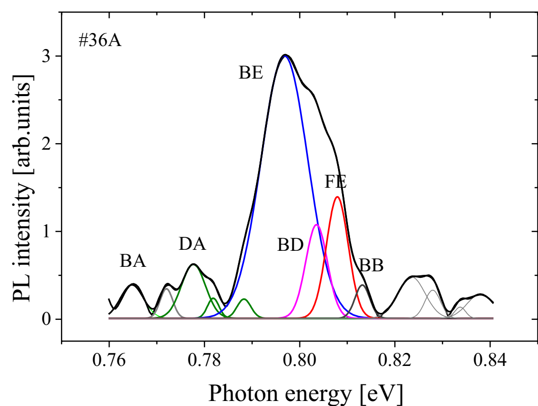

Fig. 6 PL spectra for sample #36A (GaSb/GaAs heteroepitaxial layer) at 10 K. From the fit of the measured spectra (black line) using Gaussian distribution the accurate peak positions and the energy values have been found. The free exciton peak have been identified at 0.808 eV (red line)

nature of the defects detected in GaSb/GaAs heterostructures using Laplace Deep Level Transient Spectroscopy was done by Aziz et al. [31]. He listed trap energies connected with interface states, as well as vacancies and interstitial defects.

The set B of GaSb/GaAs samples differed from set A in that, the ramp of growth temperature preceding the GaSb growth took place after the GaAs layer termination, and not during the GaAs growth. Based on the comparison of the results obtained for samples #32A and #37B it is clear that this approach provides material of better crystal and optical quality: narrower FWHM of $2\theta/\omega$ and rocking curve, stronger PL intensity (Table 5). Further improvement of a crystal quality was observed for thicker layers (#38B, #39B). The narrowest $FWHM_{2\theta/\omega}$ of 42 arcsec was obtained for the thickest layer of 5.0 µm (#39B, Fig. 7). This may be related to a thickness-dependent strain relaxation [32] or to a reduction of dislocation density in the GaSb volume. $\Delta q_z/\Delta q_x$ ratio of 0.60 [Fig. 7 (right)] higher than the one obtained for thinner 2.5 µm layer (#38B) may suggest the latter.

To verify both the arrangement and the type of dislocations at the GaSb/GaAs interface, the low and high

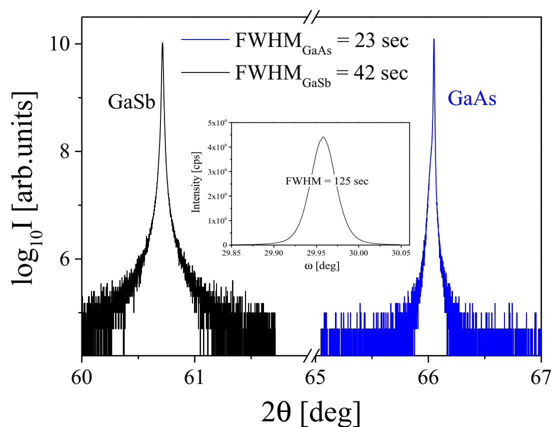

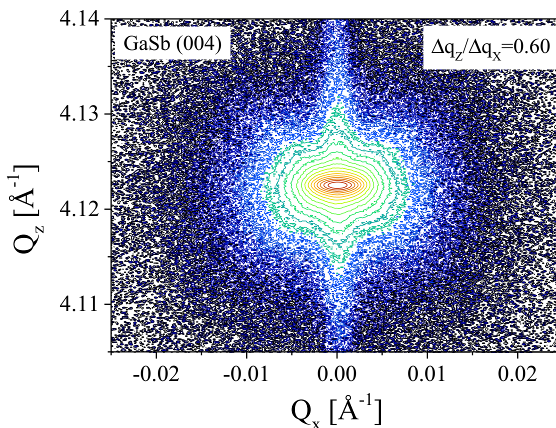

Fig. 7 (left) The $2\theta/\omega$ scan of GaSb and GaAs 004 reciprocal lattice points measured for 5.0 µm sample #39B. The lattice mismatch determined from peaks position is 78,363 ppm. The inset shows rocking curve of GaSb 004 peak. The FWHM of GaSb peak is 125 arcsec. (right) 004 reciprocal space map of GaSb peak. The $\Delta q_z/\Delta q_x$ ratio is 0.60

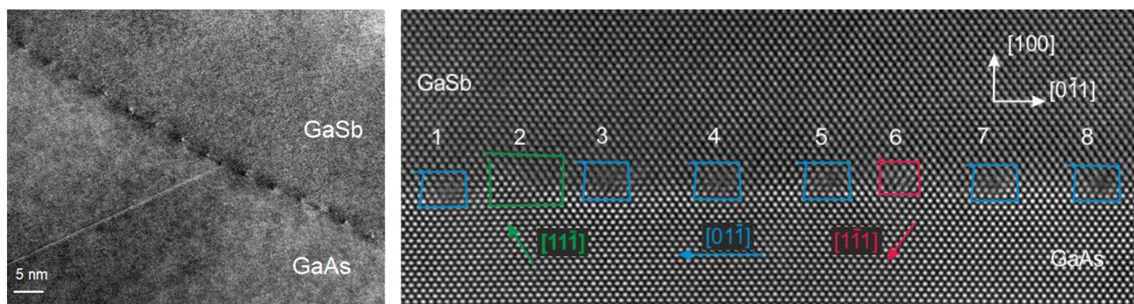

Fig. 8 Cross-sectional (left) and high-resolution (right) TEM images of GaSb/GaAs interface showing IMF array (left) and both Burger's loops around dislocations and vector's directions for sample #38B

resolution transmission electron microscopy was employed. The test was carried out for sample #38B with $\Delta q_z/\Delta q_x$ ratio of 0.59 (Fig. 8).

The cross-sectional TEM image shows the GaSb/GaAs interface along [01-1] direction. The dark spots corresponds to misfit dislocation sites. There is a spatial correlation between dislocations in the area of view. No threading dislocations or any other defects were observed in GaSb layer. The dislocation line was detected in GaAs buffer layer. The average distance between dislocations is about 5.51 nm, i.e. a little less than between the sites indicated by skipped every 14th GaAs lattice site at the GaSb/GaAs interface. The reason for that is shorter distance between 5th and 6th dislocations, which disturbed the periodicity of the dislocation array. The careful analysis of the lattice surroundings of misfit dislocations on HRTEM image allowed for determination of the type of the dislocation. Completed Burger's vector around the misfit dislocation indicates that this is a 90° one. In opposite case, the dislocation is the other type. This means that eight dislocations visible in the image are edge dislocations placed in the interface plane as Burger's vectors are elongated in [01-1] direction. One of them marked in red colour is elongated in [1-11] direction. Uncompleted Burger's vector directed in [11-1] around 2nd dislocation indicates that the dislocation is not 90°.

The effectiveness of IMF array in reduction of dislocation density may be also evaluated by the density of threading dislocations. These can be made visible on the (100) GaSb surface by etching using $FeCl_3$:HCl-based solution after chemically degreasing in acetone and isopropanol. The solution was selected after many trials of GaSb surface etching in other chemicals, for example, similar to that used by Reijnen et al. [33]—H_2O:H_2O_2:HCl and Huang et al. [25]—20% KOH solution. These attempts have provided worse results than the one with $FeCl_3$:HCl etching solution: either very defected surface did not allow for estimation of the etch pits density (EPD) or too low EPD was obtained. The images of GaSb surfaces with etch pits obtained using the scanning electron microscopy (SEM) are presented in Fig. 9.

The etch pits with triangular shape were taken into account when calculating the dislocation density. The EPD was about 4×10^7 and 4×10^6 cm^{-2} for samples #38B and #39B, respectively. This may suggest that for the GaSb layers thicker than 2.5 μm some dislocations stopped to propagate through the layer or they bended to the edge of sample and did not reach the surface. This may be an explanation of better crystal quality of thicker layer (comparison between samples #38B and #39B). The lowest EPD of 7×10^5 cm^{-2} was obtained by Huang et al. [25]. The result of 1×10^7 cm^{-2} was reached by Richardson et al. [26].

The electrical parameters measured for the thick sample #38B using Van der Pauw method (including the depletion regions of ~ 0.14 and ~ 0.20 μm at 300 and 77 K, respectively) were as follows: the hole concentration was 4.0×10^{16} cm^{-3} (2.0×10^{16} cm^{-3}) and the hole mobility was 599 cm^2/V·s (3420 cm^2/V·s) at 300 K (77 K). The similar results were obtained by Xie et al. [19] for 3.0 μm GaSb layer.

3 Summary and conclusions

The onset of IMF array formation has been investigated comprehensively. To fully relax the GaSb material grown on GaAs substrate in a volume of few monolayers, the periodic array of edge dislocation was used. This was possible after modifying growth conditions of GaAs material to meet the requirements imposed by the optimal growth conditions of GaSb material. After that IMF mode was examined based on the static diagram for GaAs surface stabilized by As_2 particles. Three sets of trials were tested for two cases of temperature reduction: either before or after the GaAs growth termination. The trials based on the subsequent temperature decreasing to 515 °C and the significant As-partial pressure reduction were used for further investigation of GaSb/GaAs interface formation. The influence of the interruption time on GaSb/GaAs heterostructure parameters was examined for the temperature decrease before and after finishing GaAs growth and for two Sb-soaking times.

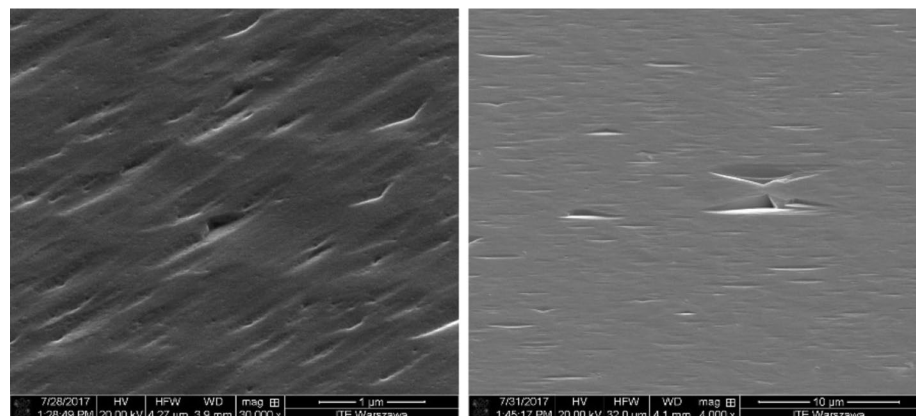

Fig. 9 The images of GaSb surfaces after etching with solution $FeCl_3$:HCl obtained using SEM for samples #38B (left) and #39B (right). The EPD was about 4×10^7 and 4×10^6 cm^{-2} for samples #38B and #39B, respectively

The strain relaxation by the array of mostly 90° dislocations at the heterointerface was diagnosed using Kaganer's parameter of $\Delta q_z/\Delta q_x$ ratio equal to 0.59. TEM investigations showed a periodic array of lattice sites with the average distance of 5.51 nm between them. The result was confirmed using Burger's circuit theory around the misfit dislocations. The completed Burger's vectors laid along the interface and identified the misfit dislocations as the edge type except for one, which was probably of mixed type (open Burger's vector).

The technological parameters used for growth of fully relaxed GaSb/GaAs heterostructure with IMF array are as follows:

(a) GaAs growth: after typical oxide desorption, substrate was heated to 615 °C and then cooled to $T_G = 580$ °C without annealing; growth rate $r_G = 1$ Å/s, V/III = 8.0; the result: 2D growth mode, 500 nm GaAs layer with roughness RMS = 5.5 Å, $FWHM_{RC}$ = 9.8 arcsec and the reduced impurity concentration at the interface.

(b) GaSb growth: $T_G = 520$ °C, $r_G = 1$ Å/s, V/III = 3.5; the result: 2D growth mode (step by step), 1.0 µm GaSb layer with roughness RMS = 1.1 Å, $FWHM_{RC}$ = 14.8 arcsec, $\frac{I_{FE}}{I_{PL}} = 0.23$.

(c) Steps for IMF mode: stop GaAs growth, decrease of the temperature to 515 °C, the reduction of As partial pressure during 3.0 min., Sb-soaking of GaAs surface during 3.0 s and GaSb growth initiation. The result: 2.5 µm GaSb layer on GaAs-buffered substrate with mostly 90° misfit dislocations periodically separated by 5.51 nm ($\Delta q_z/\Delta q_x$ = 0.59) on average. Other 2.5 µm—GaSb layer parameters: $FWHM_{2\theta/\omega}$ = 50 arcsec, $p = 4.0 \times 10^{16}$ cm^{-3} (2.0×10^{16} cm^{-3}) and $\mu = 599$ cm^2/V s (3420 cm^2/V s) at 300 K (77 K), EPD = 4×10^7 cm^{-2}. 5.0 µm—GaSb material was characterized by $\Delta q_z/\Delta q_x = 0.60$, $FWHM_{2\theta/\omega}$ = 42 arcsec, EPD = 4×10^6 cm^{-2}.

To provide the perfect periodicity of IMF array, the Sb-soaking time has to be optimized in more systematic study.

Acknowledgements This work was partially supported by the National Science Centre (NCN), Project No. 2013/11/B/ST7/04341.

Open Access This article is distributed under the terms of the Creative Commons Attribution 4.0 International License (http://creativecommons.org/licenses/by/4.0/), which permits unrestricted use, distribution, and reproduction in any medium, provided you give appropriate credit to the original author(s) and the source, provide a link to the Creative Commons license, and indicate if changes were made.

References

1. B.-M. Nguyen, D. Hoffman, P.-Y. Delaunay, M. Razeghi, Appl. Phys. Lett. **91**, 163511 (2007)
2. A. Soibel, S.B. Rafol, A. Khoshakhlagh, J. Nguyen, L. Hoeglund, S.A. Keo, J.M. Mumolo, J. Liu, A. Liao, D.Z.-Y. Ting, S.D. Gunapala, IEEE Photonics Technol. Lett. **25**(9), 875–878 (2013)
3. S. Bandara, N. Baril, P. Maloney, C. Billman, E. Nallon, T. Shih, J. Pellegrino, M. Tidrow, Infrared Phys. Technol. **59**, 18–21 (2013)
4. R.J. Malik, J.P. van der Ziel, B.F. Levine, C.G. Bethea, J. Walker, J. Appl. Phys. **59**, 3909 (1986)
5. Y.-C. Xin, L.G. Vaughn, L.R. Dawson, A. Stintz, Y. Lin, L.F. Lester, D.L. Huffaker, J. Appl. Phys. **94**, 2133 (2003)
6. E.A. Pease, L.R. Dawson, L.G. Vaughn, P. Rotella, L.F. Lester, J. Appl. Phys. **93**, 3177 (2003)
7. R.N. Kyutt, R. Scholz, S.S. Ruvimov, T.S. Argunova, A.A. Budza, S.V. Ivanov, P.S. Kopev, L.M. Sorokin, M.P. Scheglov, Phys. Solid State **35**, 372–378 (1993)
8. A. Jallipalli, G. Balakrishnan, S.H. Huang, T.J. Rotter, K. Nunna, B.L. Liang, L.R. Dawson, D.L. Huffaker, Nanoscale Res. Lett. **4**, 1458 (2009)
9. A.M. Rocher, Solid State Phenom **19/20**, 563 (1991)
10. S.V. Ivanov, P.D. Altukhov, T.S. Argunova, A.A. Bakun, A.A. Budza, V.V. Chaldyshev, YuA. Kovalenko, P.S. Kop'ev, R.N. Kutt, B.Ya Meltser, S.S. Ruvimov, S.V. Shaposhnikov, L.M. Sorokin, V.M. Ustinov, Semicond. Sci. Technol. **8**, 347 (1993)
11. A.E. Blakslee, M.M. Al-Jassim, J.M. Olson, K.M. Jones, S.M. Vernon, Mater. Res. Soc. Symp. Proc. **116**, 313 (1988)
12. M.M. Al-Jassim, T. Nishioka, Y. Itoh, A. Yamamoto, M. Yamaguchi, Mater. Res. Symp. Proc. **116**, 141 (1988)
13. A. Trampert, E. Tournie, K.H. Ploog, Appl. Phys. Lett. **66**, 2265 (1995)
14. J.C.P. Chang, T.P. Chin, J.M. Woodall, Appl. Phys. Lett. **69**, 981 (1996)
15. N.Y. Jin-Phillipp, W. Sigle, A. Black, D. Babic, J.E. Bowers, E.L. HuQuest, M. Rühle, J. Appl. Phys. **89**, 1017 (2001)
16. Y.H. Kim, J.Y. Lee, Y.G. Noh, M.D. Kim, S.M. Cho, Y.J. Kwon, J.E. Oh, Appl. Phys. Lett. **88**, 2419071 (2006)
17. A. Jallipalli, K. Nunna, M.N. Kutty, G. Balakrishnan, L.R. Dawson, D.L. Huffaker, Appl. Phys. Lett. **95**, 202107 (2009)
18. C.J.K. Richardson, L. He, P. Apiratikul, N.P. Siwak, R.P. Leavitt, Appl. Phys. Lett. **106**, 101108 (2015)
19. Q. Xie, J.E. Van Nostrand, R.L. Jones, J. Sizelove, D.C. Look, Electrical and optical properties of undoped GaSb grown by molecular beam epitaxy using cracked Sb1 and Sb2. J. Cryst. Growth **207**, 255–265 (1999)
20. E.J. Koerperick, L.M. Murray, D.T. Norton, T.F. Boggess, J.P. Prineas, Optimization of MBE-grown GaSb buffer layers and surface effects of antimony stabilization flux. J. Cryst. Growth **312**, 185–191 (2010)
21. A. Bignazzi, E. Grilli, M. Guzzi, M. Radice, A. Bosacchi, S. Franchi, R. Magnanini, Low temperature photoluminescence of tellurium-doped GaSb grown by molecular beam epitaxy. J. Cryst. Growth **169**, 450–456 (1996)
22. R. Hao, Y. Xu, Z. Zhou, Z. Ren, H. Ni, Z. He, Z. Niu, Growth of GaSb layers on GaAs (001) substrate by molecular beam epitaxy. J. Phys. D Appl. Phys. **40**, 1080–1084 (2007)
23. K. Regiński, M. Bugajski, Thin Solid Films **267**, 54–57 (1995)
24. A.S. Bracker, M.J. Yang, B.R. Bennet, J.C. Culbertson, W.J. Moore, J. Cryst. Growth **220**, 384–392 (2000)
25. S.H. Huang, G. Balakrishnan, A. Khoshahklagh, A. Jallipalli, L.R. Dawson, D.L. Huffaker, Appl. Phys. Lett. **88**, 131911 (2006)
26. C.J.K. Richardson, L. He, S. Kanakaraju, J. Vac. Sci. Technol. B **29**, 03C126 (2011)

27. Y. Wang, P. Ruterana, L. Desplanque, S.El Kazzi, X. Wallart, Strain relief at the GaSb/GaAs interface versus substrate surface treatment and AlSb interlayers thickness. J. Appl. Phys. **109**, 023509 (2011)
28. S.H. Huang, G. Balakrishnan, M. Mehta, A. Khoshakhlagh, L.R. Dawson, D.L. Huffaker, P. Li, Epitaxial growth and formation of interfacial misfit array for tensile GaAs on GaSb". Appl. Phys. Lett. **90**, 161902 (2007)
29. V.M. Kaganer, R. Köhler, M. Schmidbauer, R. Opitz, B. Jenichen, Phys. Rev. B **55**(3), 1793–1810 (1997)
30. W.J. Jing, Y.M. Sun, M.C. Wu, J. Appl. Phys. **77**, 1725 (1995)
31. M. Aziz, P. Ferrandis, A. Mesli, R.H. Mari, J.F. Felix, A. Sellai, D. Jameel, N. Al Saqri, A. Khatab, D. Taylor, M. Henini, J. Appl. Phys. **114**, 134507 (2013)
32. C.J. Reyner, J. Wang, K. Nunna, A. Lin, B. Liang, M.S. Goorsky, D.L. Huffaker, Appl. Phys. Lett. **99**, 231906 (2011)
33. L. Reijnen, R. Brunton, I.R. Grant, J. Cryst. Growth **275**, 595 (2005)